Tunable Amphiphilic Poly(Ether-Anhydride) Gel Nanoparticles for the Delivery of Hydrophobic Drugs

Zheng Wang, Zheng Cai, Qian Guo*

Summary: Biodegradable amphiphilic poly(ether-anhydride) gel nanoparticles (GNPs) with a hydrophobic crosslinked core and a hydrophilic PEG shell have been prepared from amphiphilic photo-crosslinkable ether-anhydride macromers via microemulsion photo-polymerization. The properties of the GNPs, such as degradability, size and drug-loading capacity, were investigated by tailoring the length of PEG chains in macromers from 400 to 4000 and by the addition of a hydrophobic photo-crosslinkable monomer: stearic monoacrylic anhydride (MSA). TEM showed that the GNPs were spherical in shape with a core-shell structure when MSA was added. The GNPs were used as the carriers to enhance the solubility of hydrophobic drugs. Indomethacin (IND) as a model drug was entrapped in the hydrophobic crosslinked core by an *in situ* embedding method. Results showed that IND maintained chemically intact during the formulation process, and its dissolution rate were improved compared to those of the pure IND. The GNPs prepared from PEG macromer (molecular weight: 4000) with the addition of MSA exhibited the zero-order release behavior, which is potentially useful to control the release of hydrophobic drugs.

Keywords: core-shell polymers; gel nanoparticle (GNPs); hydrophobic drug; photo-polymerization; poly(ether-anhydride)

Introduction

The poor solubility of a significant number of drugs is a substantial problem in drug delivery development. Since many new drugs happen to be hydrophobic, formulating these drugs to achieve therapeutically-effective plasma concentrations has become an overriding challenge. To increase drug dissolution efficacy, and thereby bioavailability, various formulation approaches have been developed, particularly nanosized drug delivery systems based on biodegradable polymers, such as polymer micelles,[1] liposomes,[2] microemulsions,[3] biodegradable nanoparticles[4,5] and nanogels.[6] These nanocarriers can reduce the nonspecific systemic toxicity of drugs, and allow a targeted and controlled release of drugs.

Among these nanocarriers, polymeric micelles with unique core-shell architecture have attracted much attention. The core-shell architecture is the key feature of these novel drug carriers. The hydrophobic core can solubilize lipophilic molecules, whereas the hydrated poly(ethylene glycol) (PEG) shell prevents the aggregation and protein adsorption of the micelles, and their being treated as foreign bodies by the immune system.[7,8] Because of their small size, micelles easily penetrate the intercellular spaces in body compartments (such as tumors and infracts) where the vascular system shows enhanced permeability and retention (EPR).[1] However, the disruption of micelles caused by binding on proteins in the blood stream and dilution into body fluids below critical micelle

Tianjin Key Laboratory for Modern Drug Delivery & High-Efficiency, School of Pharmaceutical Science and Technology, Tianjin University, Tianjin 300072, P. R. China
Fax: 86-022-27404018;
E-mail: wangzheng2006@tju.edu.cn

concentration (CMC) leads to burst-release of the entrapped drugs. Besides, the aggregation of micelles during storage imposes a limitation on the use of polymer micelle systems as drug carriers.[1]

Gel nanoparticles (or nanogels), which exhibit the characteristics of both nanoparticles and hydrogels, can overcome the drawbacks of micelles. They have attracted growing interest as potential delivery systems for substances such as anticancer drugs,[9,10] proteins and genes.[11,12] Some gel nanoparticles can be prepared by emulsion photo-polymerization.[9,12] This technique has several advantages over conventional polymerization, including mild and convenient reaction conditions, spatial and temporal control over polymerization, minimal heat production, low toxicity, low organic solvent levels and less by-product formation.[13]

In this study, amphiphilic photo-crosslinked poly(ether-anhydride) GNPs were designed and prepared to obtain a proper drug delivery system for hydrophobic drugs. The hydrophilicity vs. hydrophobicity, drug-loading capacity, degradation rate and release behavior of the prepared GNPs were investigated and adjusted by changing the length of PEG chains or by adding a hydrophobic reactive monomer (monoacrylated stearic anhydride, MSA). These novel GNPs have a strong potential as agents to control the release and enhance the solubility of hydrophobic drugs.

Experimental Part

Materials

Methacrylic anhydride (MA) was synthesized with a typical yield of 63% and 97% purity. A UV initiator, 2,2-dimethoxy-2-phenylacetophenone (DMPA), was obtained from Aldrich. Polyethylene glycol (PEG, average molecular weight (Mw): 4000, 2000, 400) and stearic acid were purchased in Tianjin, China, and left to dry for 24 h under vacuum. Acryloyl chloride was purchased in Shanghai, China. Indomethacin (IND) was provided by Shijiazhuang Huasheng Pharmaceutical Group Co., Ltd, China. Polyvinyl alcohol (PVA, average molecular weight ~6000, 80% hydrolyzed) was kindly supplied by Shanxi Sanwei Group Co., Ltd, China. All solvents used were of analytical grade and were redistilled before use.

Synthesis of Ether-Anhydride Macromers

Amphiphilic photocrosslinkable ether-anhydride macromers were synthesized by melt-condensation of PEG disuccinate (PEGSUC) with MA as previously described.[14] The synthetic route is shown in Scheme 1. PEGSUCs and macromers (with different molecular weight (g/mol): 4000, 2000, 400) were abbreviated as PEGSUC4K, PEGSUC2K, PEGSUC400, macromer4K, macromer2K and macromer400, respectively.

PEGSUCs with various PEG Mw were prepared from PEG and succinic anhydride. Briefly, 10 g of PEG were dissolved in 140 ml of dry toluene, and then azeotropic distilled at 110 °C to afford a 10% solution. Succinic anhydride (2.5 equivalents of PEG) was then added, and the mixture was refluxed for 5 h at 150 °C. After cooling to room temperature, the reaction mixture was filtered and concentrated under vacuum. The residue was dissolved in saturated $NaHCO_3$ and then filtered. The filtrate was acidified to pH 3-4 by means of 5% hydrochloric acid. The resulting solution was extracted twice with chloroform. The chloroform fractions were mixed and dried overnight with anhydrous Na_2SO_4, followed by filtration and vacuum-concentration. The PEGSUC4K and PEGSUC2K thus obtained were precipitated, whereas PEGSUC400 was phase-separated in a large excess of ether. The final products were then dried for 24 h at 40 °C under vacuum.

The amphiphilic photo-crosslinkable ether-anhydride macromers were synthesized from the above prepared PEGSUCs and MA. The reaction conditions were slightly modified according to the literature.[14] Briefly, 2 g of PEGSUC were charged into a round-bottomed flask under

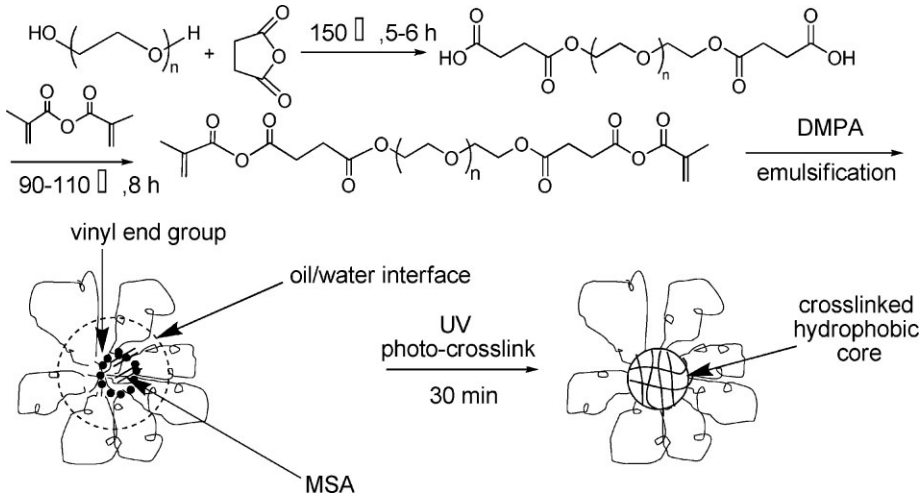

Scheme 1.
Synthesis of the ether-anhydride macromer and the formation of GNPs.

a nitrogen atmosphere. An excess of MA was then added into the flask to obtain a 10% (w/v) polymer solution. The reaction was carried out for 8 hours at 90-110 °C. After cooling to room temperature, the dimethacylated macromer4K and macromer2K were precipitated in a large excess of ether and filtered. They were further purified by re-dissolution in dichloromethane (DCM) and re-precipitation by the addition of ether. The macromer400 was phase-separated in a large excess of hexane. All the obtained macromers were dried for 3 h under vacuum and were immediately used in the preparation of GNPs.

PEGSUCs and ether-anhydride macromers (molecular weight: 400) were characterized by FT-IR and ^{1}H-NMR. FT-IR spectra were recorded by a FTS3000 spectrometer (BIO-RAD, USA). ^{1}H-NMR was conducted using D_2O as the solvent and a Varian INOVA spectrometer (500 MHz).

Synthesis of Monoacrylated Stearic Acid (MSA)

9.95 g (0.035 mol) stearic acid and 7.22 ml (0.05 mol) Et_3N were dissolved in 50 ml DCM and stirred at 0 °C for 60 min under nitrogen. 4.06 ml (0.05 mol) acryloyl chloride was then added dropwise. Stirring was continued at a reduced temperature for 5.5 h, followed by vacuum filtration to remove the precipitated triethylammonium chloride. The filtrate was washed sequentially with saturated $NaHCO_3$ (60 ml × 2) and distilled H_2O (60 ml × 2). The solution was dried over Na_2SO_4, and DCM was removed under vacuum. The viscous liquid obtained was precipitated twice in an ethyl ether/ ethanol (2/3) mixture. The resulting yellow solid (MSA) was obtained in 82% yield, and was characterized by ^{1}H-NMR and. FT-IR (cm^{-1}) as shown in Figure 1 and Figure 2.

Preparation of Gel Nanoparticles

In a typical experiment, 1 g ether-anhydride macromer, MSA (6% w/w macromer, if added) and the initiator DMPA (3% w/w macromer) were dissolved in 10 ml DCM. The mixture was then added dropwise to a 40 ml 2.5% PVA aqueous solution under mechanical stirring to afford an emulsion that was then sonicated for 10 minutes using a probe sonicator (JY88 Crusher, Ningbo Scientz Biotechnology Co., China) with a power output of 200 w in pulse mode. The resulting O/W microemulsion was exposed to a low-tensity UV-light (3.5 mw/cm^2) and

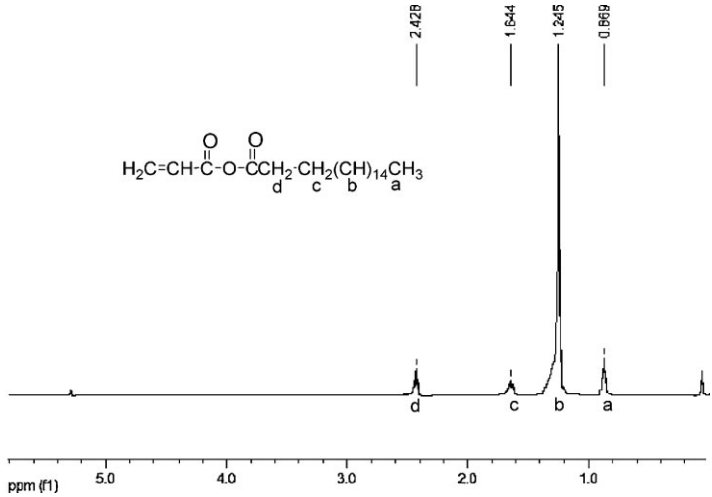

Figure 1.
^{1}H-NMR spectrum of monoacrylated stearic acid (MSA) in D_2O.

irradiated for 60 min, under moderate mechanical stirring (400 rpm). After illumination, the DCM was removed under continuous stirring for 2 h. The gel nanoparticles obtained at this stage were collected by centrifugation (30 minutes, 22,000 rpm, 4 °C) using an Avanti J-20XPI centrifuge (Beckman Coulter, USA), washed three times to remove the excess emulsifier and the unreacted macromer, and finally lyophilized for 48 hours. GNPs prepared from the different macromers, with or without the addition of MSA, were abbreviated as GNP4K, GNP2K, GNP400, GNP4K-MSA, GNP2K-MSA and GNP400-MSA.

Indomethacin (IND) was embedded into the GNPs and the preparation process was exactly the same as above, except that 400 mg IND were added in 10 ml DCM. The IND loaded GNP was abbreviated as GNP + IND.

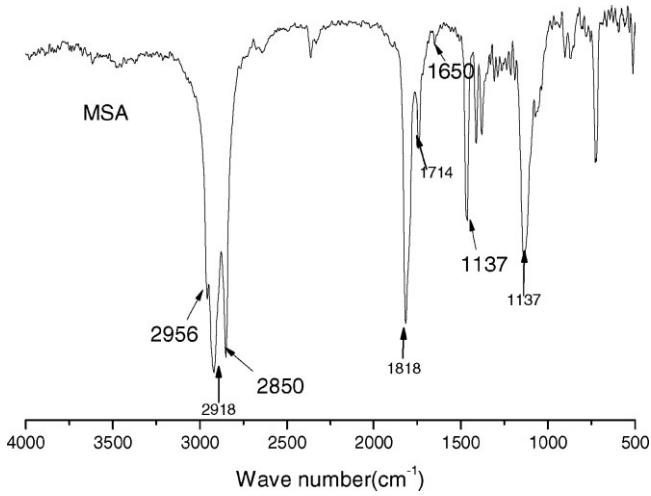

Figure 2.
FT-IR spectrum of of monoacrylated stearic acid (MSA).

Characterization of the Polymer Particles

The morphology of gel nanoparticles was observed by transmission electron microscopy (TEM, JEM-100CX, JEOL, Japan). A drop of GNP suspension was placed on the copper electron microscopy grids and dried at room temperature for several hours before examination.

The hydrodynamic size of nanoparticles was determined by laser particle analyzer (LPA, BI-90 Plus, Brookhaven inst, Huntsville, NY, USA) at a fixed angle of 90° at 25 °C. In short, the GNP suspension (before lyophilization) was sonicated to form a uniform dispersion. Size distribution was given by the polydispersity index.

The crystallinity of GNPs and the morphology of IND in GNPs were evaluated by wide-angle X-ray powder diffraction (RAD-IC, Rigaku, Japan). In brief, dried powder samples were attached directly to a sample holder with double-sided adhesive tape. The measurement was performed at a scan rate of 8° degree/min under Cu/K-α1 radiation (40 kV, 200 mA) between 3° and 60° of 2θ.

Degradation of GNPs *in vitro*

The lyophilized GNPs were re-dispersed in 5 ml phosphate-buffered saline (PBS, 0.1 M, pH 7.4). The suspensions were then put into a dialysis bag (with a molecular weight cutoff of 12 000, Shanghai Green Bird Co., China) and incubated in 200 ml PBS at 37 °C in a shaking water bath with a shaking speed of 100 rpm. Samples were removed, lyophilized and weighed at various time intervals to monitor the cumulative weight loss of GNPs, and the buffer was refilled at each time interval. A ''Blank'' PBS in a dialysis membrane without GNPs was maintained at the same time for comparison.

Drug Contents (DC), Encapsulation Efficacy (EE) and Drug Release Behavior

The drug contents of GNPs were determined as follows: 10 mg of lyophilized GNPs + IND were dispersed in 20 ml of 50% methanol (v/v), sonicated for 1.5 h, and the supernatants were isolated by centrifugation at 22000 rpm for 30 min. After passing through a 0.22 μm syringe millipore filter, the filtrates were diluted to some extent and the IND concentration was measured by UV/vis spectrophotometer (SHIMADZU, UV-2450, Japan). The drug contents (DC) and encapsulation efficiency (EE) were calculated according to the following equations (1) and (2):

$$\mathrm{DC}(\%, \mathrm{W/W}) = \frac{\text{Mass of drug in GNPs}}{\text{Mass of dry GNPs}} \times 100\% \quad (1)$$

$$\mathrm{EE}(\%, \mathrm{W/W}) = \frac{\text{Mass of drug in GNPs}}{\text{Mass of drug fed initially}} \times 100\% \quad (2)$$

The IND-loaded GNPs were re-dispersed in 5 ml PBS, then placed in a dialysis membrane bag with a molecular weight cutoff 12 000 (Shanghai Green Bird Co., China), and put into 200 ml of PBS. The entire system was incubated at 37 °C in a shaking water bath with a shaking speed of 100 rpm. At predetermined time intervals, 5 ml aliquots were withdrawn and replaced by 5 ml fresh buffer solution maintained at the same temperature. These aliquots were immediately passed through a 0.22 μm filter and assayed for IND concentration by UV/vis spectrophotometer. As a reference system for dissolution tests, commercially-available indomethacin crystalline powders (30-80 μm) were used.

Results and Discussion

Synthesis and Characterization of Macromers

With slight modification, the photo-cross-linkable ether-anhydride macromers with different molecular weights of PEGs were successfully synthesized according to the literature.[14] The reaction temperature was adjusted according to the PEG chain length. A trace amount of inhibitors was used to protect the double bonds remaining in the macromers after reaction at high temperature. Table 1 shows the results of

Table 1.
The characterization and yield of PEGSUCs and photo-crosslinkable ether-anhydride macromers

	Appearance	Melting point (°C)	Yield (%)
PEGSUC4K	white solid	57.9-59.0	93.7
PEGSUC2K	white solid	47.2-49.9	87.8
PEGSUC400	yellow viscous liquid	–	78.2
macromer4K	white solid	48.3-49.7	83.3
macromer2K	white solid	38.6-40.1	93.9
macromer400	yellow viscous liquid	–	90.4

PEGSUC precursors and the macromers indicating the successful synthesis.

The macromers were analyzed by ^{1}H-NMR and FT-IR as shown in Figures 3 and 4, respectively. Figure 3 (B) shows that the methylene protons in the succinate moity adjacent to the anhydride bond (peak b') in the macromers were shifted to 2.544 ppm, while the chemical shift of the methylene protons in the PEGSUC was at 2.536 ppm (peak b in Figure 3 (A). The ratio of the peak integral of the two methacrylate protons (peak e' and f') to those of the methylene protons adjacent to the ester bond (peak d) revealed that most carboxylic acid had been converted into the mixed anhydride of PEGSUC and MA. The vinyl group coming from the methacrylate of the macromer was further characterized by FT-IR spectroscopy as shown in Figure 4. The absorption band of the OH group at the terminal of PEGSUC at about 3400 cm^{-1} disappeared, whereas an absorption at 1637 cm^{-1} that represents the C = C in the vinyl groups appeared in the macromer spectrum confirming the presence of the dimethacrylate in PEGSUC.

Preparation and Characterization of Gel Nanoparticles

Preparation of Gel Nanoparticles

Amphiphilic poly(ether-anhydride) gel nanoparticles were formulated via microemulsion photo-polymerization as shown in Scheme 1. The process parameters were optimized with different conditions as the followings: organic to aqueous phase volume (O/W) ratio is 1:5; surfactant PVA concentration is 2.5%; sonication time is 10 min; sonication pulse mode is 50% and the hydrophobic stearic acid

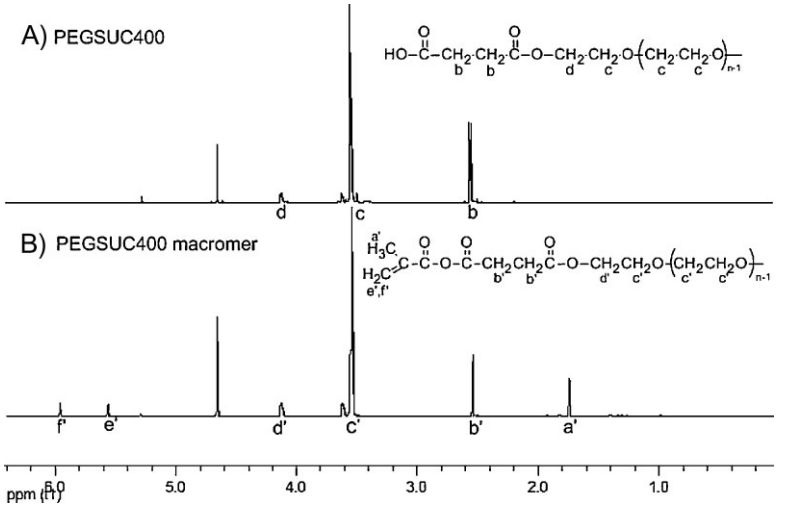

Figure 3.
^{1}H-NMR spectrum of PEG disuccinate (PEGSUC400) and PEGSUC400 macromer in D_2O.

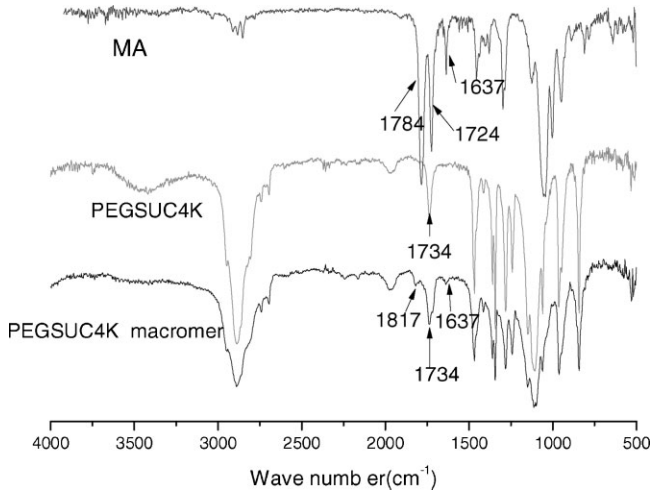

Figure 4.
FT-IR spectrum of methacrylic anhydride (MA), PEG4K disuccinate (PEGSUC4K) and PEGSUC4K macromer.

addition is 5% w/w macromer.. In this paper, the effects of different PEG macromers and the addition of MSA and IND on the particle size of GNPs were investigated.

As shown in Table 2, the effective diameter of GNPs increased as the molecular weight of PEG chain decreased. The macromers became less hydrophilic with a shorter PEG chain, which results in less macromer leaking from the oil phase into the outer aqueous phase during the formation of O/W microemulsion. With more macromers participated in the photo-polymerization, the size of GNPs was consequently increased. Furthermore, the size of GNPs enlarged with the addition of hydrophobic MSA probably because the viscosity of the organic phase increased and the hydrophobic interaction between the monomers enhanced at the same time. Large O/W microemulsion droplets were then formed leading to the increase of the GNP size.

Table 2.
The particle size and polydispersity index (PI) of GNPs by laser particle analyzer

GNPs	Effective diameter (nm)	PI
GNP4K	462.5	0.005
GNP2K	521.8	0.238
GNP400	671.9	0.497
GNP (4K-MSA)[a]	633.2	0.261
GNP (2K-MSA)[a]	566.0	0.322
GNP (400-MSA)[a]	670.9	0.318

[a]prepared from PEG macromer (4000, 2000, 400) with MSA (6% w/w).

Morphology of GNPs

The morphology and structure of GNPs was characterized by transmission electron microscopy (TEM). As shown in Figure 5, the gel nanoparticles were spherical in shape. Interestingly, with the addition of MSA in macromers, a distinct core-shell structure in Figure 5 (B, D) was observed, which indicates that a copolymerization of ether-anhydride macromer with MSA has taken place in the emulsion droplet due to the presence of a vinyl functional-group at the end of MSA leading to the crosslinked hydrophobic core. This core-shell structure of GNPs could be tuned by tailoring the PEG length in macromer as shown in Figure 5 (B, D). The formation of the structure appears to be similar to that of the nanogel from diacrylated amphiphilic PLA-PEG-PLA prepared by Lee *et al.*[9] because of the amphiphilic composition of the ether-anhydride macromer and the core-shell structure of GNPs obtained with the addition of MSA.

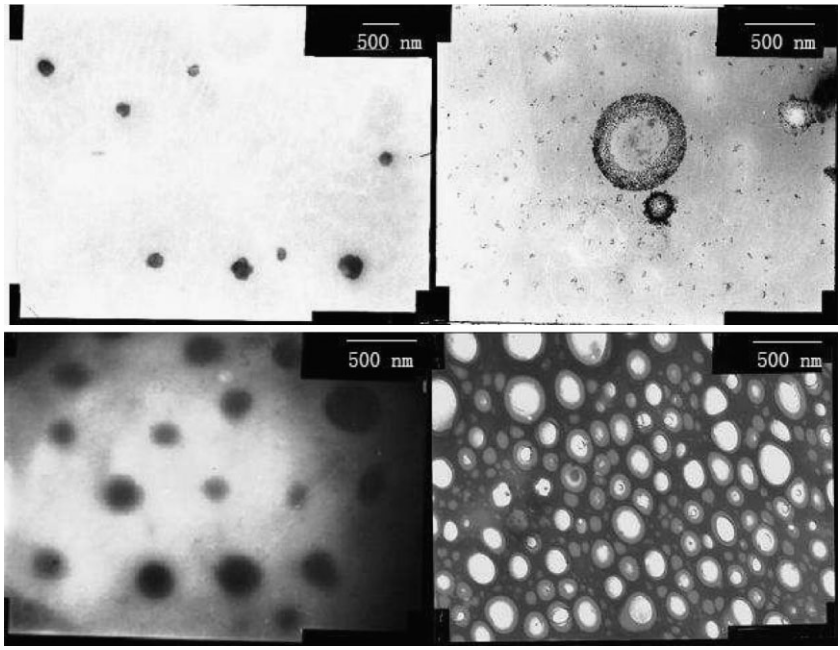

Figure 5.
The TEM microphotographs of GNPs, (A): GNP 400, ×19k; (B): GNP (400-MSA), ×29K; (C): GNP4K, ×36k; (D): GNP (4K-MSA), ×29k.

In vitro Degradation of GNPs

As shown in Figure 6, all the GNPs prepared from ether-anhydride macromers were biodegradable and degraded into PEG, poly(methacrylic acid) with low molecular weight and succinate, which are biocompatible according to the report by B. S. Kim *et al*..[14] The degradation rate could be tailored by changing the length of PEG. The longer the PEG chain in the GNPs, the faster the GNPs degraded. The reason might be due to the fact that the

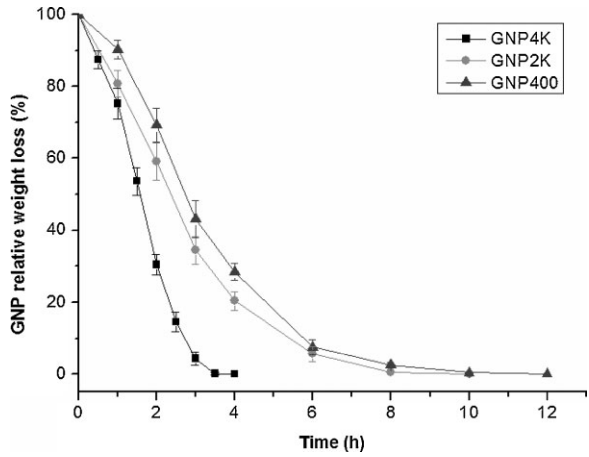

Figure 6.
The *in vitro* degradation behavior of GNP4K, GNP2K and GNP400.

longer PEG chains entailed a more hydrophilic GNP shell and a lower crosslinking density of the core networks, which in turn resulted in an easier infiltration of water molecules into the GNP networks leading to the faster hydrolysis of anhydride and ester bonds. On the other hand, the degradation rate was affected by the size of the GNPs. The smaller the size of nanoparticles was, the faster their degradation exhibited, which is in good agreement with the results reported by D. Klose *et al.*.[15]

Drug Loading in the Gel Nanoparticles

An *in situ* UV photo-crosslinking technology was adopted to prepare the drug-loaded GNPs. During the preparation process, sonication and UV illumination had been used to form O/W microemulsion and the polymerization was irradiated. To verify that the selected drug could withstand these processes and maintain its chemical integrity during the preparation process, HPLC analysis and FTIR measurements were conducted (data not shown). The results indicated that IND had been incorporated in the nanoparticles without any deterioration.

The drug contents (DC) and entrapment efficiency (EE) of the drug-loaded GNPs prepared from the different monomers were analyzed. As shown in Figure 7A, the DC and EE of IND-loaded GNPs

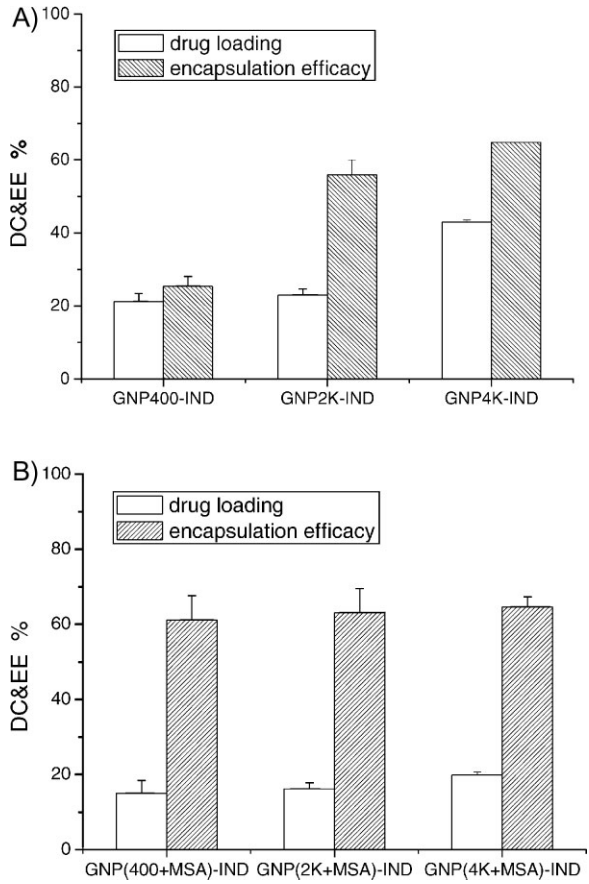

Figure 7.

A. The effect of PEG length on the drug content (DC) and encapsulation efficacy (EE) of GNPs + IND. B. The effect of the addition of MSA on the drug content (DC) and encapsulation efficacy (EE) of GNPs + IND.

prepared from ether-anhydride macromers with different molecular weight of PEG increased with the increase of PEG chain. The highest EE and DC were obtained with GNP4K + IND. This might be attributed to the curing time of the gel particles. Since the macromers with higher molecular weight of PEGs feature a relatively lower density of double bounds in the oily phase, the curing time is shorter, and thereby less of the drug diffused into the external water phase. In addition, the lower crosslinking density of these GNPs with longer PEG chains may provide a larger space to entrap the drugs within the internal core network.

The positive result of using a hydrophobic monomer on the EE of GNPs was shown in Figure 7B. The EE of IND loaded in GNPs containing MSA was relatively high (about 65%) for all the GNPs prepared from the different molecular weight of macromers with the addition of MSA. Actually, the fact that the incorporation of hydrophobic additives in micelles can greatly increase the EE of poorly water-soluble drugs was reported by Ashok, B. *et al.*,[16] and was also established by our own lab. It is conceivable that the introduction of hydrophobic MSA might increase the viscosity of the oil phase, as well as enhance the hydrophobic interaction between the drug and the hydrophobic core, both of which can contribute to preventing the drug from leaking out, and therefore improving the encapsulation of the drug in GNPs. However, the DC of IND was decreased to some extent due to the fact that the MSA may occupy some space of the hydrophobic core.

The crystallinity of the drug carriers can affect the drug loading capacity. Nanoparticles with high crystallinity may have low drug loading efficacy, whereas their amorphous phase is more likely to accommodate drug molecules. Thus the crystallinity of GNP (2K-MSA) drug carrier was investigated by X-ray diffraction. As shown in Figure 8, there was no obvious diffraction absorption of GNP (2K-MSA), which indicates that GNP (2K-MSA) has a certain potential for the accommodation of hydrophobic drugs. The morphology of IND entrapped in the GNPs was also investigated by X-ray diffraction as shown in Figure 8 (E, F). The representative crystal peaks of IND were disappeared for GNP (2K-MSA) + IND, which indicates that IND was amorphously or molecularly distributed in the crosslinked networks of GNPs. Since the amorphous state of drug

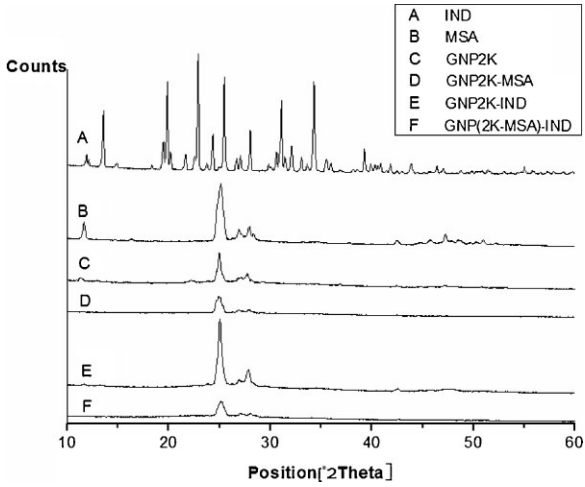

Figure 8.
The X-ray diffraction analysis of (A): IND; (B): MSA; (C): GNP2K; (D): GNP (2K-MSA); (E): GNP2K + IND; and (F): GNP (2K-MSA) + IND.

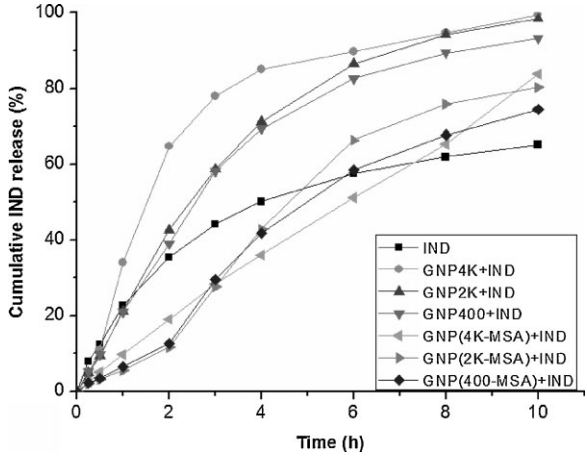

Figure 9.
The *in vitro* release behavior of GNPs + IND.

exhibits a faster dissolution rate than the crystal state, these novel gel nanoparticles may be effective to improve the dissolution rate of the poorly soluble drugs.

The *in vitro* release behavior of different samples of GNPs + IND and pure IND were investigated as shown in Figure 9. Compared to pure IND, the three samples of GNPs + IND prepared from ether-anhydride macromers exhibited markedly faster dissolution rates, probably due to the higher surface area and the amorphous state of the drug (as confirmed by X-ray diffraction). The drug-release rate increased with the increase of PEG molecular weight. Since the release rate is controlled by both the diffusion rate of drug from the carriers into the outer aqueous phase and the degradation rate of carriers, GNPs with longer PEG chains were more hydrophilic and their core networks had lower crosslinking density, which endow water more apt to penetrate into the networks. Therefore, the drug could dissolve and diffuse more easily out of the carrier. On the other hand, GNPs with longer PEG chains exhibited faster degradation rates and the drug would be completely released as the carriers degraded. More than 93% of the amount of drugs entrapped into the three GNPs + IND was released. However, when MSA was added into the GNPs, the dissolution rate dropped severely, and IND could not be released completely, probably on account of the enhanced hydrophobic core and the strong hydrophobic interaction between IND and the crosslinked core. Interestingly, the release of the drug from GNP (4K-MSA) + IND followed zero-order kinetics, which might be useful for developing novel controlled-release drug carriers.

Conclusion

Biodegradable amphiphilic poly(ether-anhydride) gel nanoparticles (GNPs) with a hydrophobic crosslinked core and a hydrophilic PEG shell structure were formulated from amphiphilic photo-crosslinkable ether-anhydride macromers via microemulsion photo-polymerization. The hydrophobicity/hydrophilicity, degradability and drug-loading capacity of GNPs were adjusted by changing the length of PEG chains and by adding the hydrophobic monomer MSA. GNPs prepared with the addition of MSA featured a spherical and distinct core-shell structure. With the decrease of particle size, the degradation rate increased. The DC and EE rose with the length of PEG chains increased in GNPs. Conversely, the addition of MSA

increased the particle size, raised EE and reduced the dissolution rate. The most interesting finding was that the release of the drug from GNP (4K-MSA) + IND followed zero-order kinetics, which, with further modification, has the potential to control the release of drugs. The dissolution data demonstrated that the drug dissolution rate is closely related to the hydrophobicity/hydrophilicity, crystallinity and degradability of GNPs. These factors can be tuned by tailoring the length of PEG chains and the hydrophobicity of the core by means of the addition of hydrophobic MSA.

Acknowledgements: The authors are grateful to the financial support from Natural Science Foundation of China (20674055), Natural Science Foundation of Tianjin, China (05YFJMJC11200) and Starting Foundation of Tianjin University. The authors also thank Dr. Kang Zhao's research group for providing instrumental analysis and useful discussions.

[1] G. Gaucher, M. H. Dufresne, V. P. Sant, N. Kang, D. Maysinger, J. C. Leroux, *J. Control. Release* **2005**, *109*, 169.
[2] Y. Koda, M. T. Liang, J. T. Blanchfield, I. Toth, *Int. J. Pharm.* **2008**, *356*, 37.
[3] A. A. Date, M. S. Nagarsenker, *Int. J. Pharm.* **2008**, *355*, 19.
[4] J. Pan, S. S. Feng, *Biomaterials* **2008**, *29*, 2663.
[5] C. Chen, C. H. Yu, Y. C. Cheng, P. H. Yu, M. K. Cheung, *Biomaterials* **2006**, *27*, 4804.
[6] T. G. Van Thienen, J. Demeester, S. C. De Smedt, *Int. J. Pharm.* **2008**, *351*, 174.
[7] A. V. Kabanov, I. R. Nazarova, I. V. Astafieva, E. V. Batrakova, V. Y. Alakhov, A. A. Yaroslavov, V. A. Kabanov, *Macromolecules* **1995**, *28*, 2303.
[8] R. Nagarajan, *Polym. Adv. Technol.* **2001**, *12*, 23.
[9] W. C. Lee, Y. C. Li, I. M. Chu, *Macromol. Biosci.* **2006**, *6*, 846.
[10] S. V. Vinogradov, E. Kohli, A. D. Zeman, *Pharm. Res.* **2006**, *23*, 920.
[11] D. Missirlis, N. Tirelli, J. A. Hubbell, *Langmui.* **2005**, *21*, 2605.
[12] N. Morimoto, T. Endo, M. Ohtomi, Y. Iwasaki, *Akiyoshi, Macromol. Biosci.* **2005**, *5*, 710.
[13] K. T. Nguyen, J. L. West, *Biomaterials* **2002**, *23*, 4307.
[14] B. S. Kim, J. S. Hrkach, R. Langer, *J. Polym. Sci.* **2000**, *38*, 1277.
[15] D. Klose, F. Siepmann, K. Elkharraz, J. Siepmann, *Int. J. Pharm.* **2008**, *354*, 95.
[16] B. Ashok, L. Arleth, R. P. Hjelm, I. Rubinstein, H. Onyuksel, *J. Pharm. Sci.* **2004**, *93*, 2476.

